Accepted Manuscript

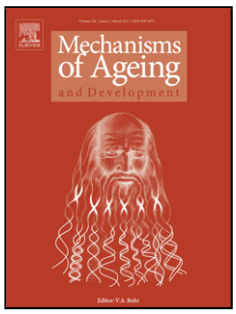

Title: Identification of survival-promoting OSIP108 peptide variants and their internalization in human cells

Author: Sara Verbandt Sónia Troeira Henriques Pieter Spincemaille Peta J. Harvey Gursimran Chandhok Vanessa Sauer Barbara De Coninck David Cassiman David J. Craik Bruno P.A. Cammue Kaat De Cremer Karin Thevissen

PII: S0047-6374(16)30129-4
DOI: http://dx.doi.org/doi:10.1016/j.mad.2016.07.013
Reference: MAD 10879

To appear in: *Mechanisms of Ageing and Development*

Received date: 25-3-2016
Revised date: 30-6-2016
Accepted date: 30-7-2016

Please cite this article as: Verbandt, Sara, Henriques, Sónia Troeira, Spincemaille, Pieter, Harvey, Peta J., Chandhok, Gursimran, Sauer, Vanessa, Coninck, Barbara De, Cassiman, David, Craik, David J., Cammue, Bruno P.A., Cremer, Kaat De, Thevissen, Karin, Identification of survival-promoting OSIP108 peptide variants and their internalization in human cells.Mechanisms of Ageing and Development http://dx.doi.org/10.1016/j.mad.2016.07.013

Identification of survival-promoting OSIP108 peptide variants and their internalization in human cells

Sara Verbandt[1*], Sónia Troeira Henriques[2*], Pieter Spincemaille[1,3], Peta J. Harvey[2], Gursimran Chandhok[4], Vanessa Sauer[4], Barbara De Coninck[1,5], David Cassiman[6], David J. Craik[2], Bruno P.A. Cammue[1,5#], Kaat De Cremer[1,5§] and Karin Thevissen[1§]

[1]Centre of Microbial and Plant Genetics, CMPG, KU Leuven, Kasteelpark Arenberg 20, box 2460, 3001 Leuven, Belgium

[2]Institute for Molecular Bioscience, University of Queensland, Brisbane, QLD, 4072, Australia

[3]Department of Laboratory Medicine, University Hospital Gasthuisberg, Herestraat 49, 3000 Leuven, Belgium

[4]Clinic for Transplantation Medicine, Münster University Hospital, Albert-Schweitzer-Campus 1, Building A14, D-48149 Münster, Germany

[5]Department of Plant Systems Biology, VIB, Technologiepark 927, 9052 Ghent, Belgium

[6]Department of Hepatology and Metabolic Center, University Hospital Gasthuisberg, Herestraat 49, 3000 Leuven, Belgium.

*both authors contributed equally

[§]Shared last author

#Corresponding author. Mailing address: CMPG, Kasteelpark Arenberg 20, 3001 Leuven, Belgium. Phone: +32 16329682. Fax: 32-16321966. E-mail: bruno.cammue@biw.kuleuven.be

Running title: Structure-activity relationship study of OSIP108

Highlights

- OSIP108 activity is improved by substitution of Val4, Leu5, Gln6 and Gly7 by charged residues or Pro
- Substitutions of Cys3 and Arg9 most negatively affect OSIP108 activity
- OSIP108[G7P] is the most active variant among 190 tested
- OSIP108 and OSIP108[G7P] are highly flexible in solution
- OSIP108 and OSIP108[G7P] internalize into HeLa cells

Abstract

The plant-derived decapeptide OSIP108 increases tolerance of yeast and human cells to apoptosis-inducing agents, such as copper and cisplatin. We performed a whole amino acid scan of OSIP108 and conducted structure-activity relationship studies on the induction of cisplatin tolerance (CT) in yeast. The use of cisplatin as apoptosis-inducing trigger in this study should be considered as a tool to better understand the survival-promoting nature of OSIP108 and not for purposes related to anti-cancer treatment. We found that charged residues (Arg, His, Lys, Glu or Asp) or a Pro on positions 4-7 improved OSIP108 activity by 10% or more. The variant OSIP108[G7P] induced the most pronounced tolerance to toxic concentrations of copper and cisplatin in yeast and/or HepG2 cells. Both OSIP108 and OSIP108[G7P] were shown to internalize equally into HeLa cells, but at a higher rate than the inactive OSIP108[E10A], suggesting that the peptides can internalize into cells and that OSIP108 activity is dependent on subsequent intracellular interactions. In conclusion, our studies demonstrated that tolerance/survival-promoting properties of OSIP108 can

be significantly improved by single amino acid substitutions, and that these properties are dependent on (an) intracellular target(s), yet to be determined.

Keywords: OSIP108, apoptosis-inducers, structure activity relationship study, survival, cellular internalization

1. Introduction[1]

Programmed cell death, or apoptosis, is essential for the function and development of multicellular organisms (Kerr et al., 1972). However, excessive apoptosis can lead to degenerative pathologies, such as Alzheimer's, Parkinson's, Huntington's and Wilson's disease (Butterfield, 2002; Jenner, 2003; Portera-Cailliau et al., 1995; Strand et al., 1998). As the life quality of patients that suffer from these disorders is largely impaired, elucidation of the detrimental mechanistic backgrounds that lead to these diseases and discovery of novel therapies are of utmost importance. Of relevance, anti-apoptotic compounds have been proposed as potential therapeutics for treatment of these diseases (Friedlander, 2003; Mattson, 2000; Thompson, 1995).

Owing to the highly conserved apoptotic pathways in eukaryotic cells, yeast (*Saccharomyces cerevisiae*) is an ideal eukaryotic model organism to study apoptosis, and information found in yeast can in many cases be directly translated to mammalian cells (Carmona-Gutierrez et al., 2010; Fröhlich et al., 2007). Hence, various yeast

[1] Abbreviations in order of appearance: SAR, structure-activity relationship; CT, cisplatin tolerance; MTT, 3-(4,5-Dimethyl-2-thiazolyl)-2,5-diphenyl-2H-tetrazolium bromide; AUC, area under the curve; TB, Trypan blue; MCT-2, minimal peptide concentration required to increase CT of the culture by 2-fold

models have been developed to study the above mentioned neurodegenerative diseases, mainly by overexpressing disease-inducing proteins that can form toxic aggregates and cause apoptosis, such as α-synuclein, amyloid-β and huntingtin, for studying Parkinson's, Alzheimer's and Huntington's diseases (Bharadwaj et al., 2010; Flower et al., 2005; Meriin et al., 2002), respectively (reviewed in (Khurana and Lindquist, 2010; Winderickx et al., 2008)). In addition, a yeast model for the rare disease Wilson's disease is also available. The latter is a condition characterized by excessive hepatic copper accumulation, resulting in apoptosis of hepatocytes, but also in neurodegeneration (Huster, 2010), and is caused by mutations in the copper transporter ATP7B (Ferenci, 2006; Forbes and Cox, 1998). As such, overexpression of ATP7B in a yeast mutant devoid of its orthologue Ccc2p, restored copper tolerance of the mutant (Hung et al., 1997).

Yeast models can be used to study the molecular mechanisms leading to the described pathologies, but they can also aid in drug discovery through screening and identification of survival-promoting molecules and elucidation of their modes of action (Griffioen et al., 2006; Johnson et al., 2008; Verbandt et al., 2016; Winderickx et al., 2008). For instance, using a copper-toxicity yeast model for Wilson's disease (Spincemaille et al., 2014b), we have previously identified a potent anti-apoptotic peptide, OSIP108, derived from the plant *Arabidopsis thaliana* (De Coninck et al., 2013). This decapeptide increases the tolerance of yeast and human cells to apoptosis-inducing compounds such as copper and cisplatin (Spincemaille et al., 2014a, 2014b). Moreover, OSIP108 also decreases copper-induced hepatotoxicity in zebrafish larvae, showing the potential of this peptide to treat hepatotoxicity in Wilson's disease (Spincemaille et al., 2014c). A preliminary structure-activity relationship (SAR) study of OSIP108 in the presence of cisplatin showed that the D-stereoisomer of OSIP108 and some cyclized variants have

an identical cisplatin tolerance (CT)-promoting activity on yeast cells compared to OSIP108 (Spincemaille et al., 2014a).

In this study we aim to identify structural features important for survival-promoting properties of OSIP108 and to optimize its activity. To achieve this goal, we have performed a detailed SAR analysis of OSIP108 using a whole amino acid replacement scan, in which every single amino acid was replaced with the other 19 amino acids. The success of this approach was demonstrated in a previous study, using the same amino acid replacement scan, in which we could demonstrate that OSIP108's antibiofilm activity was increased by introducing positively charged amino acids, whereas replacement of Arg9 by 17 out of 19 amino acids resulted in a reduction or even complete abolishment of this activity (Delattin et al., 2014b). In the present study, we used cisplatin as apoptosis-inducing trigger, as our high-throughput screening did not allow the use of copper. The latter is most relevant as causative agent of Wilson Disease, but the copper concentrations needed to induce yeast PCD cause cell aggregation under our bioscreen-based screening conditions (unpublished data). As cisplatin is used in the treatment of cancer, a peptide that promotes cisplatin tolerance can obviously never be considered for therapeutic applications in cancer settings. So, the cisplatin-based screening setup used here should only be regarded as a tool to better understand the survival-promoting nature of the OSIP108 peptide.

Hence, in this study, we evaluated the CT-promoting activity of the OSIP108 variants and examined the potential of the best OSIP108 variant to increase copper-tolerance of yeast and human cells. In addition, we assessed potential internalization of OSIP108 and some variants into human cervical cancer (HeLa) cells, and compared three-dimensional structures of OSIP108 and its most active variant to further understand the SAR of this peptide regarding its survival-promoting properties.

2. Materials and methods

2.1. Materials and microorganisms

The *Saccharomyces cerevisiae* yeast strain (BY4741) was cultured in synthetic complete (SC) medium (0.77 g/L complete amino acid supplement mixture (CSM) (Bio 101 Systems); 6.7 g/L yeast nitrogen base without amino acids (YNB); 20 g/L glucose). OSIP108 (MLCVLQGLRE) and the peptide variants (amino acid scan, double substitutions) were obtained from Pepscan (Lelystad, The Netherlands) with crude purity (< 70%). In addition, OSIP108 and OSIP108[G7P] were also obtained in 98% pure preparations (Pepscan). Of relevance, 98% pure OSIP108 and OSIP108[G7P] showed equal survival-promoting activity on yeast treated with $CuSO_4$ compared to the crude peptide preparations (data not shown), justifying the use of crude peptide preparations throughout this manuscript. Cis-diamminedichloroplatinum (II) (Cisplatin), $CuSO_4.5H_2O$ and $CuCl_2$ were purchased from Sigma Aldrich (St. Louis, USA). Peptides (20 mM) and cisplatin (50 mM) were dissolved in dimethyl sulfoxide (DMSO). HeLa (human cervix epitheloid carcinoma cells) were cultured in Dulbecco's modified Eagle's medium (DMEM) (Gibco, Invitrogen) supplemented with 10% (v/v) of fetal bovine serum and 1% (w/v) penicillin/streptomycin. HepG2 cells (human hepatocellular carcinoma cells) (ATCC, Rockville, USA) were grown in RPMI media (Lonza) supplemented with 10 % fetal calf serum, 100 U/mL penicillin and 100 µg/mL streptomycin. Cell lines were cultured using standard cell culture conditions (37ºC, 5% CO_2 in humidified atmosphere). 3-(4,5-Dimethyl-2-thiazolyl)-2,5-diphenyl-2H-tetrazolium bromide (MTT) was purchased from Sigma Aldrich.

2.2. Yeast CT assay

An overnight yeast culture in SC was diluted to OD600 of 0.1 in fresh SC and treated with 2.5% DMSO (control) or 250 µM cisplatin with or without 100 µM of the peptides. Yeast growth was subsequently monitored by recording the OD600 with a bioscreen C MBR (Oy Growth Curves Ab, Ltd, Helsinki, Finland) every 15 minutes for 44 h. Experiments were performed at 30°C, while shaking continuously at medium amplitude.

From the OD600 measurements, growth curves were plotted as OD600 values vs. time. To estimate the effect of a peptide-treatment on the growth of the cultures in the presence of a sublethal cisplatin dose (250 µM), we calculated a CT-score, which is the ratio of the area under the curve (AUC) of a peptide-treated culture to AUC of the untreated control (see supplementary figure S1 for CT-score calculation). To compare the potency of selected OSIP108 variants, dose response curves containing CT-scores vs. peptide concentration (12.5 µM- 100 µM) were plotted. MCT-2 values, i.e. the minimum concentration of the peptide necessary to increase the CT-score of a cisplatin treated culture by 2-fold, were determined for each of the OSIP108 variants. A graphical representation of the MCT-2 value is provided in supplementary figure S2.

2.3. Yeast copper survival assay

Yeast survival in presence of 1.75 mM $CuSO_4$ upon treatment with either control (2% DMSO) or peptide (100 µM) was evaluated as before (Spincemaille et al., 2014b).

2.4. HepG2 copper survival assay

Viability of HepG2 cells in presence of 0.75 mM $CuCl_2$ treated with either peptide (5 µM- 100 µM) or control (1% DMSO) was assessed as previously described

(Spincemaille et al., 2014b). Briefly, HepG2 cells were seeded in a 96-well plate and incubated with control (1% DMSO) or peptide (5 µM-100 µM). Following 16 h preincubation, cells were incubated in new culture medium containing 0.75 mM $CuCl_2$ upon treatment with control or peptide. Cell viability was determined after 48 h by MTT staining and calculated as a percentage of untreated cells.

2.5. HeLa copper survival assay

HeLa cells were seeded in a 96-well plate at 10^4 cells/well and incubated with control (1% DMSO) or peptide (5 µM- 50 µM). Following 16 h preincubation, cells were incubated in new culture medium containing 0.4 mM $CuCl_2$ upon treatment with control or peptide. Cell viability was determined after 24 h by MTT staining and calculated as a percentage of untreated cells.

2.6. NMR analysis

OSIP108 or OSIP108[G7P] (~1 mg) were dissolved in 550 µL of 10% D_2O/90% H_2O and the pH adjusted to 3.0 for NMR experiments. Spectra were recorded at 298 K on a Bruker Avance-500 or an Avance-600 spectrometer. 2D NMR experiments included TOCSY (total correlation spectroscopy, mixing time of 80 ms) and ROESY (rotating frame nuclear Overhauser effect spectroscopy, spin lock of 200 ms). Chemical shifts were referenced to internal 2,2-dimethyl-2-silapentane-5-sulfonate (DSS).

2.7. Internalization of OSIP and of its variants into HeLa cells

OSIP108 and its variants were labeled with Alexa Fluor® 488 sulfodichlorophenol ester (Life technologies) through an amide bond (Torcato et al., 2013). Briefly, peptide (0.5 mg) solubilized in sodium bicarbonate buffer (100 mM, pH 8, 90 µL) was incubated with dye (0.5 mg) solubilized in DMSO (10 µL), with N,N-

diisopropylethylamine (DIPEA; 1 μL) and with the reducing agent tris(2-carboxyethyl)phosphine (TCEP; 1 μL of 20 mM stock) and incubated for 3 h at room temperature. Labeled peptide was separated from unlabeled peptide by RP-HPLC. OSIP108, OSIP108[G7P] and OSIP108[E10A] were labeled at the N-terminal amine, whereas OSIP108[M1K], OSIP108[R9K] and OSIP108[E10K] were labeled through the side chain amine of the Lys residue. Each peptide had a single label and was purified to >95% as checked by LC-MS. Peptide stock solutions were prepared in DMSO and the peptide concentration determined following the absorbance of Alexa Fluor® 488 at 495 nm (ε_{495} = 71,000 $M^{-1}.cm^{-1}$).

HeLa cells were seeded in 24-well plates (10^5 cells per well) and following attachment overnight, internalization of fluorescently-labeled peptides was monitored by flow cytometry as described before (Huang et al., 2015; Torcato et al., 2013). Briefly, HeLa cells were incubated with labeled OSIP108 or OSIP108 variants (2 – 16 μM) for 1 h at 37ºC in fresh medium without serum (to avoid peptide degradation). Fluorescently-labeled TAT, a gold standard cell-penetrating peptide, and TAT-G, a non-penetrating analogue (D'Souza et al., 2014) were included as controls. Final DMSO background was kept below 8% (v/v) for all peptide concentrations tested; the potential effect of DMSO in the internalization was examined by comparing the internalization of TAT in the absence/presence of different percentages of DMSO. Cells were washed with cold phosphate buffer saline (PBS) to remove non-internalized peptide, harvested from the plate by trypsinization, centrifuged at 500 *g* at 4ºC, washed and re-suspended in cold PBS. Fluorescence emission (excitation at 488 nm and emission at 530 nm with a band pass of 30 nm) of treated cells (10.000 cells per sample) was monitored by flow cytometry (BD FACSCanto™ II) before and after addition of trypan blue (TB, 160

μg/mL). DMSO did not affect the overall uptake of TAT or TAT-G in the conditions tested (up to 8% (v/v) of DMSO).

2.8. Statistical analysis

Values are represented as mean with standard error of the mean (SEM). The data were analysed using GraphPad Prism 6.0. P value < 0.05 was considered to be statistically significant. Prior to all statistical analysis, normality was tested using Shapiro-Wilk normality test ($\alpha = 0.05$).

3. Results

3.1. SAR study of OSIP108 on yeast in the presence of cisplatin

The apoptosis-inducing effect of cisplatin on the model yeast *S. cerevisiae* was quantified by scoring the cisplatin tolerance (CT) of a treated yeast culture as detailed in the Materials and Methods section. Treatment of yeast with 100 μM OSIP108 in the absence of cisplatin did not affect the growth (CT-score = 1) (data not shown), whereas treatment with 250 μM cisplatin reduced the growth by 90% (CT-score = 0.10 ± 0.03). Yeast cultures treated with 250 μM cisplatin and 100 μM OSIP108 showed a CT-score of 0.55 ± 0.04. Thus, the addition of 100 μM OSIP108 increased growth of a 250 μM cisplatin-treated culture by 5.5-fold.

The effect of the 190 OSIP108 variants on yeast growth in the presence of cisplatin was tested and compared to that of OSIP108 and a heat map was constructed (Fig. 1), in which all amino acid-substituted OSIP108 variants are ranked relative to average CT-score of OSIP108 for each individual amino acid. From this heat map, we can conclude that CT-promoting activity can be most improved (up to 30%) by replacing the amino acids on position 4 – 7. Out of 19 possible amino acid substitutions Val4 can be improved by 13 amino acid substitutions, Leu5 by 15, Gln6 by 10 and Gly7 by six,

respectively. A different view of these data is obtained by visualizing the amino acid replacement scan in a second heat map in which the amino acids are colour-coded based on their main characteristics (supplementary figure S3). In general, replacing the amino acids on positions 4-6 with positively (Lys, Arg or His) or negatively (Asp or Glu) charged amino acids or with Pro results in improved CT-promoting activity (except for introduction of His on position 6, Asp on position 4 and Glu on position 5 which affect CT-score by less than 10%). Also substitution of Gly7 by Pro and Asp results in improved CT-promoting activity. Additionally, introduction of positively charged amino acids on other positions (Lys on position 2, 7 and 8; and Arg on position 10) results in improved CT-promoting activity, while introduction of Lys on position 3 and His on position 8 negatively affects CT-promoting activity. In contrast, substitution of Cys3 by nine amino acids, Leu8 by six amino acids or Arg9 by eight out of the 19 amino acids leads to a reduction (of at least 10%) of the average CT-score compared to native OSIP108, showing the importance of Cys3, Leu8 and Arg9 (Fig. 1). Other positions (Met1, Leu2 and Glu10) are less prone to affection of the CT-score. Interestingly, introduction of aromatic residues rarely results in improved CT-promoting activity (only substitution of Leu2 by Tyr) and often results in reduced CT-promoting activity (e.g. substitution of Cys3, Gly7, Leu8, Arg9 and Glu10 by Phe) (supplementary figure S3).

3.2. OSIP108[G7P] is characterized by improved CT-promoting activity

To further optimize the amino acid sequence of OSIP108 for maximal activity, we selected 18 OSIP108 variants with improved CT-promoting activity (Fig. 1), being L2G, L2K, L2Y, V4H, V4K, V4S, L5A, L5H, L5S, Q6E, Q6K, Q6P, G7D, G7K, G7P, L8K, L8M and E10R, and performed dose response curves (data not shown). (For the

sake of simplicity OSIP108 variants are referred to by the substitution, e.g., "G7P" instead of OSIP108[G7P]). These variants were selected based on two criteria: (i) being one of the three best variants conferring CT for each position; and (ii) increase of at least 10% in average CT-score (Fig. 1). We calculated the MCT-2 (minimal peptide concentration required to increase average CT-score by 2-fold) from the dose-response curves and results are shown in Table 1. The MCT-2 value of OSIP108 is 44.5 ± 3.4 µM.

Based on MCT-2 values, the best substitutions for each position are L2G, V4H, L5S, Q6P, G7P, L8K and E10R. The most promising single substituted OSIP108 variant was G7P with MCT-2 of 9.2 ± 1.4 µM (Table 1). To assess whether we could further increase the activity of the G7P variant, we combined the above best substitutions with G7P into double substituted variants, resulting in L2G/G7P, V4H/G7P, L5S/G7P, Q6P/G7P, L8K/G7P, E10R/G7P and tested their CT-promoting activity at different concentrations (Fig. 2). We compared sample MCT-2 values using one-way ANOVA followed by a Tukey-multiple comparison test ($\alpha = 0.05$). Interestingly, we found that no further improvements in CT-promoting activity of G7P could be obtained based on SAR of OSIP108 (Table 1). In fact, a combination of the improved variant G7P with E10R (i.e., G7P/E10R) resulted in a significant reduction of the CT-promoting activity compared to that of the single G7P substitution (P value = 0.00036); the MCT-2 value of G7P/E10R was equal to that of OSIP108 (P value = 1) (Table 1).

In conclusion, we showed that G7P is characterized by the most improved CT-promoting activity of all tested variants, and that on average a 4.8-fold lower concentration of G7P, as compared to OSIP108, is required to obtain a similar CT-improvement of the yeast culture.

3.3. G7P shows improved survival-promoting activity on yeast

To assess whether G7P can also increase tolerance of yeast to another apoptosis-inducer, being copper, we assessed survival of yeast cells treated with a toxic $CuSO_4$ dose (1.75 mM) in the presence of OSIP108 or G7P. This toxic copper dose was selected based on survival determination of yeast cultures treated with a range of copper doses as this dose decreased survival of the yeast culture to approximately 30%. (data not shown). The colony forming units (CFUs) were counted and survival percentages were calculated in comparison to the untreated control (no copper/no peptide). We found that the activity of G7P in this setup was significantly increased compared to that of OSIP108 (P value = 0.0124): treatment with G7P increased the survival of yeast cells in the presence of toxic copper by 1.7-fold (from 31% to 53%), but only 1.3-fold (from 31% to 41%) when treated with the OSIP108 (Fig. 3A).

3.4. G7P shows improved survival promoting activity on HepG2 cells

To translate the yeast-based data to a higher eukaryotic cell model we assessed the effect of OSIP108 and G7P on viability of HepG2 cells (human hepatocellular carcinoma cells) treated with copper. The choice for copper-induced toxicity in HepG2 cells is based on the direct correlation between copper-induced toxicity in hepatocytes and the human Wilson's disease (Huster, 2010). We first treated HepG2 cells with different copper concentrations and selected 0.75 mM $CuCl_2$ for further experiments, as this concentration reduced HepG2 viability by more than 50% (Fig. 3B). Treatment with OSIP108 and G7P increased survival compared to the copper-treated control at all peptide doses (5 µM– 50 µM) (supplementary figure S4; P value < 0.05). Note that treatment of untreated HepG2 cells (without copper) with OSIP108 did not affect survival. At a peptide dose of 20 µM, we measured significant improvement in survival

by treatment with G7P compared to treatment with OSIP108 (Fig. 3B; P value = 0.013). Whereas viability of HepG2 cells was approx. 40% after challenge with 0.75 mM $CuCl_2$, treatment with 20 µM OSIP108 or G7P increased viability to 56% and 66%, respectively (Fig. 3B). When comparing treatment of HepG2 cells with both peptides at higher peptide dose (50 µM), we observed no difference in survival of cell cultures after treatment with G7P compared to OSIP108 (both peptides increased viability up to almost 70%). Using lower peptide concentrations (5 µM and 10 µM), we measured a substantial, however not significant ($\alpha = 0.05$), increase in survival by treatment with G7P compared to native OSIP108 (see supplementary figure S4). These results show improved survival-promoting activity of G7P as compared to OSIP108 on HepG2 cells in the presence of toxic copper doses.

To gain further insight in the structure of OSIP108 and G7P, we performed NMR analysis of OSIP108 and of the improved variant G7P. The 1D ^{1}H NMR spectrum of both these peptides showed poor dispersion in the amide region, indicative of limited secondary structure. Secondary chemical shift analysis (Fig. 4) also indicated that neither peptide adopted any secondary structure and that both OSIP108 and G7P were highly flexible and 'random coil' in nature. Replacing the Gly at position 7 by a Pro did not increase the peptide's rigidity nor induce any local structure.

3.5. OSIP108 and G7P are internalized into HeLa cells, whereas inactive E10A is not

To obtain more insight in the activity of OSIP108, we assessed potential cell internalization of OSIP108. To this end, we used a N-terminally labelled OSIP108 with Alexa fluor®488 and assessed its internalization into HeLa cells, the most common model cell used to conduct internalization assays. The gold standard cell-penetrating

peptide TAT was included as a positive control, and its derivative TAT-G (in which positively-charged residues are replaced with Gly) was used to evaluate non-specific cellular internalization. Trypan blue (TB), a membrane-impermeable dye, was added to quench the fluorescence of cells with compromised membranes and/or the fraction of membrane-bound peptide (Torcato et al., 2013). The mean fluorescence emission signal of peptide-treated cells obtained after addition of TB is proportional to the amount of peptide internalized into cells, whereas the percentage of fluorescent cells gives information on the fraction of viable cells which have peptide internalized.

Using flow cytometry we found that OSIP108 is internalized into HeLa cells in non-permeabilising conditions: after one hour incubation all cells (>98%) became fluorescent (Fig. 5A, left panel), and the mean fluorescence signal was significantly higher than in cells treated with the negative control TAT-G (P value = 0.029, Fig. 5B). To examine whether the CT-promoting activity of OSIP108 correlates with the ability to internalize into cells, we monitored the internalization rate of two OSIP108 variants E10A and G7P, which respectively are inactive and active to promote CT in yeast as compared to OSIP108 (Fig. 5C). The inactive E10A showed a significantly decreased internalization rate (P value = 0.007 at 16 μM), Fig. 5C), whereas the more active G7P showed identical internalization efficiency rate compared to that of OSIP108 (P value > 0.99999 at 16 μM). Internalization of the peptides suggests (an) intracellular interaction(s) to promote survival. However, when measuring activity of OSIP108 and G7P on HeLa cells, we observed a significant reduction in cell survival of peptide-treated cells in the absence of copper (supplementary figure S5). This reduction was even more pronounced for G7P compared to native OSIP108 (P value = 0.0051 at 20 μM). In the presence of 0.4 mM copper, the reduced survival was only substantial for G7P-treated HeLa cells (supplementary figure S5).

4. Discussion

OSIP108 is a plant-derived decapeptide with anti-apoptotic properties (Spincemaille et al., 2014b). Its therapeutic potential was previously demonstrated as it can increase survival of several eukaryotic cell models for Wilson's disease, such as a copper-treated Chinese Hamster Ovary (CHO) cell line expressing either *ATP7B* or *ATP7B*^{H1069Q}, or a copper-treated U87 glioblastoma cell line (Spincemaille et al., 2014c). We previously also translated these findings to a zebrafish larvae model for Wilson's disease. Injection of OSIP108 in zebrafish larvae reduced the copper-induced aberrancies in liver morphology and hepatotoxicity showing the potential of this peptide and potentially more active variants as lead peptides for the development of a novel peptide-based therapy for Wilson's disease.

The main aim of the present study was to identify important amino acids that are relevant for the tolerance-/survival-promoting activity of OSIP108. Thus, we have performed a detailed SAR analysis of OSIP108, using a whole amino acid replacement scan. We found that the CT-promoting activity of OSIP108 can be most improved (up to 30%) by replacing the amino acids on position 4 – 7 (Val4, Leu5, Gln6 and Gly7, respectively). In general, replacing these amino acids with positively (Lys, Arg or His) or negatively (Asp or Glu) charged amino acids or with Pro, results in improved CT-promoting activity. Additionally, introduction of positively charged amino acids on other positions (Lys on position 2, 7 and 8; and Arg on position 10) also results in improved CT-promoting activity. Potentially, the introduction of charged residues enhances the solubility of the peptide, improves its cellular uptake and/or interaction with its target. The presence of a Pro residue might affect the secondary structure of the peptide, however, this was not confirmed for the G7P variant which was as flexible in solution as the native OSIP108. Interestingly, introduction of aromatic residues at

different positions results in reduced CT-promoting activity. Introduction of aromatic residues has been shown to impose steric blocking and as such might hinder interactions of the peptide with (a) possible interaction partner(s) (Bai et al., 1993). Substitutions of Cys3 and Arg9 most negatively affect the CT-promoting activity. These findings are in agreement with our previous studies in which a cyclic OSIP108 variant with a disulphide bond between Cys3 and a C-terminally added Cys (Cys11) showed reduced CT-promoting activity (Spincemaille et al., 2014a), and with the study of (Delattin et al., 2014b), as explained below.

We previously showed that OSIP108 can also inhibit formation of *Candida albicans* biofilms (Delattin et al., 2014c). *C. albicans* is the predominant human fungal pathogen and accounts for 35% of invasive fungal infections (Lewis et al., 2013). *C. albicans* cells can also grow as a surface-attached biofilm, e.g., on catheters and heart valves, thereby causing recurrent systemic infections (Cuéllar-Cruz et al., 2012; Mayer et al., 2013), which are in general resistant to most antimycotics (De Cremer et al., 2015; Delattin et al., 2014a). In the search for novel antibiofilm molecules, we previously identified OSIP108 as a new antibiofilm peptide (Delattin et al., 2014c). To get more insight into important amino acids that are linked to OSIP108's antibiofilm activity, we also performed a SAR using the same amino acid replacement scan (Delattin et al., 2014b). In line with the observations in our current study, the antibiofilm activity of OSIP108 could be increased by introducing positively charged amino acids whereas replacement of Arg9 by 17 out of 19 amino acids resulted in a reduction or even complete abolishment of this activity. However, it seems that some amino acid substitutions have a different effect on OSIP108's activity in both setups. For example, substitution of Leu5 by 15 out of 19 leads to improved CT-promoting activity whereas 12 of these amino acid improvements lead to a decreased antibiofilm activity of

OSIP108. To better understand the apparent differences in amino acid requirements for optimal activity of OSIP108 in both setups, it will be essential to determine the corresponding OSIP108 target(s).

Moreover, the present study indicates that site-specific amino acid substitutions can significantly improve the CT- and survival-promoting activity of OSIP108. Studying OSIP108 variants with single and double substitutions allowed us to select the single substitution OSIP108 variant G7P as the best OSIP108 variant with regard to CT- and survival-promoting potential. OSIP108 G7P is characterized by a 4.8-fold decrease in MCT-2 on yeast cells treated with 250 µM cisplatin as compared to OSIP108. Note that G7P-based double substitution variants (like G7P/E10R) displayed even reduced CT-promoting potential, showing that combination of single substitutions that positively affect the CT-promoting activity (e.g. G7P and E10R) does not necessarily translate into a further activity improvement. A full SAR analysis of G7P should be performed to either confirm the superiority of this variant or to further improve its activity.

NMR analysis showed that both OSIP108 and its G7P variant are highly flexible in solution. As such, the improved activity of G7P cannot be attributed to alterations in its structure. This improved activity of G7P was confirmed in yeast and human HepG2 cultures treated with copper, pointing to the generally improved tolerance-promoting activity of this peptide variant. In human HepG2 cells, both OSIP108 and G7P were able to increase copper-affected cell survival from 40% to almost 70%, a maximal threshold that was reached at lower concentrations for G7P, illustrating its superiority over native OSIP108 in this cell line.

Our future research is aimed at discovering the target of OSIP108 and its active variants, which could be both intracellular or extracellular. To discriminate between those two options, we investigated whether native OSIP108, the improved G7P variant and an

inactive variant (E10A) could be internalized into human HeLa cells. Interestingly, we could demonstrate that OSIP108 and G7P are internalized in HeLa cells, in contrast to the E10A variant. Note that similar internalization of peptides in both HepG2 and HeLa cells has been reported (Fang et al., 2013; Richard et al., 2005). These data suggest that the absence of E10A activity is correlated with its compromised uptake. At this moment, it is unclear whether the impeded internalization of E10A is due to a specific change in the C-terminal sequence or the difference in overall charge (caused by the substitution of a Glu residue). The latter is unlikely, since several substitutions of this position (e.g by Gly, Ile, Val and Leu) affecting overall charge in the same way as E10A were still active. Internalization of OSIP108 and G7P suggests that activity is conferred via intracellular interactions, leading to a survival benefit in HepG2 cells but reduced survival of HeLa cells. This inconsistency might be explained by differences within the reaction of both cell types to the stressor (copper), or absence/inactivity of targets necessary for the OSIP108 rescuing mechanisms. Indeed, HeLa cells are reported to be sensitive to the tumor necrosis factor-related apoptosis-inducing ligand (TRAIL) while HepG2 cells are TRAIL-resistant cancer cells, potentially explaining the observed difference in this apoptosis context (Shi et al., 2005).

It is currently not clear how uptake of small peptides like OSIP108 could be mediated in yeast. Yeast possesses transporters for di-/tripeptides (encoded by *PTR2* and *DAL5*) (Cai et al., 2007; Homann et al., 2005) and for tetra-/pentapeptides (encoded by *OPT1* and *OPT2*) (Aouida et al., 2009; Bourbouloux et al., 2000). However, a transport system for decapeptides has not yet been found in *S. cerevisiae*, but assessing the mode of uptake of OSIP108 might add information on such systems.

In conclusion, we found improved activity of G7P as compared to OSIP108 in both yeast and human HepG2 cells. Both peptides are equally flexible in solution and are as

efficiently internalized in HeLa cells. Based on all these findings, we will focus our future research on the identification of the intracellular OSIP108 target. As the internalization efficiency of OSIP108 and G7P were found to be the same, and they are both unstructured, the improved activity of G7P is likely to relate to its improved interaction with (an) intracellular target(s), yet to be identified.

5. Acknowledgements

S.V. and P.S. acknowledge receipt of a predoctoral grant of IWT-Vlaanderen; K.T. acknowledges the receipt of a mandate of Industrial Research Fund, KU Leuven. B.D.C. and K.D.C. acknowledge the receipt of a postdoctoral fellowship from FWO Vlaanderen. D.C. is a fundamental clinical researcher with the FWO Vlaanderen. D.J.C. is supported by an Australian Research Council Laureate Fellowship (FL150100146). S.T.H. is funded by a project grant from NHMRC (APP1084965). We are grateful for access to the facilities of the Queensland NMR Network.

6. References

Aouida, M., Khodami-Pour, A., Ramotar, D., 2009. Novel role for the Saccharomyces cerevisiae oligopeptide transporter Opt2 in drug detoxification. Biochem. Cell Biol. 87, 653–661. doi:10.1139/o09-045

Bai, Y., Milne, J.S., Mayne, L., Englander, S.W., 1993. Primary structure effects on peptide group hydrogen exchange. Proteins Struct. Funct. Bioinforma. 17, 75–86. doi:10.1002/prot.340170110

Bharadwaj, P., Martins, R., Macreadie, I., 2010. Yeast as a model for studying Alzheimer's disease. FEMS Yeast Res. 10, 961–969. doi:10.1111/j.1567-1364.2010.00658.x

Bourbouloux, A., Shahi, P., Chakladar, A., Delrot, S., Bachhawat, A.K., 2000. Hgt1p, a high affinity glutathione transporter from the yeast Saccharomyces cerevisiae. J. Biol. Chem. 275, 13259–13265. doi:10.1074/jbc.275.18.13259

Butterfield, D.A., 2002. Amyloid β-peptide (1-42)-induced oxidative stress and neurotoxicity: implications for neurodegeneration in Alzheimer's disease brain. A review. Free Radic. Res. 36, 1307–1313. doi:10.1080/1071576021000049890

Cai, H., Hauser, M., Naider, F., Becker, J.M., 2007. Differential regulation and substrate preferences in two peptide transporters of Saccharomyces cerevisiae. Eukaryot. Cell 6, 1805–1813. doi:10.1128/EC.00257-06

Carmona-Gutierrez, D., Eisenberg, T., Büttner, S., Meisinger, C., Kroemer, G., Madeo, F., 2010. Apoptosis in yeast: triggers, pathways, subroutines. Cell Death Differ. 17, 763–773. doi:10.1038/cdd.2009.219

Cuéllar-Cruz, M., Vega-González, A., Mendoza-Novelo, B., López-Romero, E., Ruiz-Baca, E., Quintanar-Escorza, M., Villagómez-Castro, J., 2012. The effect of biomaterials and antifungals on biofilm formation by Candida species: a review. Eur. J. Clin. Microbiol. Infect. Dis. 31, 2513–2527. doi:10.1007/s10096-012-1634-6

De Coninck, B., Carron, D., Tavormina, P., Willem, L., Craik, D.J., Vos, C., Thevissen, K., Mathys, J., Cammue, B.P., 2013. Mining the genome of Arabidopsis thaliana as a basis for the identification of novel bioactive peptides involved in oxidative stress tolerance. J. Exp. Bot. 64, 5297–5307. doi:10.1093/jxb/ert295

De Cremer, K., Staes, I., Delattin, N., Cammue, B., Thevissen, K., De Brucker, K., 2015. Combinatorial drug approaches to tackle Candida albicans biofilms. Expert Rev. Anti Infect. Ther. 13, 973–984. doi:10.1586/14787210.2015.1056162

Delattin, N., Cammue, B.P., Thevissen, K., 2014a. Reactive oxygen species-inducing antifungal agents and their activity against fungal biofilms. Future Med. Chem. 6, 77–90. doi:10.4155/fmc.13.189

Delattin, N., De Brucker, K., Craik, D.J., Cheneval, O., De Coninck, B., Cammue, B.P., Thevissen, K., 2014b. Structure-activity relationship study of the plant-derived decapeptide OSIP108 inhibiting Candida albicans biofilm formation. Antimicrob. Agents Chemother. 58, 4974–4977. doi:10.1128/AAC.03336-14

Delattin, N., De Brucker, K., Craik, D.J., Cheneval, O., Fröhlich, M., Veber, M., Girandon, L., Davis, T.R., Weeks, A.E., Kumamoto, C.A., 2014c. Plant-Derived Decapeptide OSIP108 Interferes with Candida albicans Biofilm Formation without Affecting

Cell Viability. Antimicrob. Agents Chemother. 58, 2647–2656. doi:doi: 10.1128/AAC.01274-13.

D'Souza, C., Henriques, S.T., Wang, C.K., Craik, D.J., 2014. Structural parameters modulating the cellular uptake of disulfide-rich cyclic cell-penetrating peptides: MCoTI-II and SFTI-1. Eur. J. Med. Chem. 88, 10–18. doi:10.1016/j.ejmech.2014.06.047

Fang, B., Guo, H.Y., Zhang, M., Jiang, L., Ren, F.Z., 2013. The six amino acid antimicrobial peptide bLFcin6 penetrates cells and delivers siRNA. FEBS J. 280, 1007–1017. doi:10.1111/febs.12093

Ferenci, P., 2006. Regional distribution of mutations of the ATP7B gene in patients with Wilson disease: impact on genetic testing. Hum. Genet. 120, 151–159. doi:10.1007/s00439-006-0202-5

Flower, T.R., Chesnokova, L.S., Froelich, C.A., Dixon, C., Witt, S.N., 2005. Heat shock prevents alpha-synuclein-induced apoptosis in a yeast model of Parkinson's disease. J. Mol. Biol. 351, 1081–1100. doi:10.1016/j.jmb.2005.06.060

Forbes, J.R., Cox, D.W., 1998. Functional characterization of missense mutations in ATP7B: Wilson disease mutation or normal variant? Am. J. Hum. Genet. 63, 1663–1674. doi:10.1086/302163

Friedlander, R.M., 2003. Apoptosis and caspases in neurodegenerative diseases. N. Engl. J. Med. 348, 1365–1375. doi:10.1056/NEJMra022366

Fröhlich, K.U., Fussi, H., Ruckenstuhl, C., 2007. Yeast apoptosis—from genes to pathways. Semin. Cancer Biol. 17, 112–121. doi:10.1016/j.semcancer.2006.11.006

Griffioen, G., Duhamel, H., Van Damme, N., Pellens, K., Zabrocki, P., Pannecouque, C., Van Leuven, F., Winderickx, J., Wera, S., 2006. A yeast-based model of α-synucleinopathy identifies compounds with therapeutic potential. Biochim. Biophys. Acta BBA-Mol. Basis Dis. 1762, 312–318. doi:10.1016/j.bbadis.2005.11.009

Homann, O.R., Cai, H., Becker, J.M., Lindquist, S.L., 2005. Harnessing natural diversity to probe metabolic pathways. PLoS Genet 1, e80. doi:10.1371/journal.pgen.0010080

Huang, Y.-H., Chaousis, S., Cheneval, O., Craik, D.J., Henriques, S.T., 2015. Optimization of the cyclotide framework to improve cell penetration properties. Front. Pharmacol. 6, 1–7. doi:10.3389/fphar.2015.00017

Hung, I.H., Suzuki, M., Yamaguchi, Y., Yuan, D.S., Klausner, R.D., Gitlin, J.D., 1997. Biochemical characterization of the Wilson disease protein and functional expression in the yeast Saccharomyces cerevisiae. J. Biol. Chem. 272, 21461–21466. doi:10.1074/jbc.272.34.21461

Huster, D., 2010. Wilson disease. Best Pract. Res. Clin. Gastroenterol. 24, 531–539. doi:10.1016/j.bpg.2010.07.014

Jenner, P., 2003. Oxidative stress in Parkinson's disease. Ann. Neurol. 53, S26–S38. doi:10.1002/ana.10483

Johnson, B.S., McCaffery, J.M., Lindquist, S., Gitler, A.D., 2008. A yeast TDP-43 proteinopathy model: Exploring the molecular determinants of TDP-43 aggregation and cellular toxicity. Proc. Natl. Acad. Sci. 105, 6439–6444. doi:10.1073/pnas.0802082105

Kerr, J.F., Wyllie, A.H., Currie, A.R., 1972. Apoptosis: a basic biological phenomenon with wide-ranging implications in tissue kinetics. Br. J. Cancer 26, 239–257. doi:10.1111/j.1365-2796.2005.01570.x

Khurana, V., Lindquist, S., 2010. Modelling neurodegeneration in Saccharomyces cerevisiae: why cook with baker's yeast? Nat. Rev. Neurosci. 11, 436–449. doi:10.1038/nrn2809

Lewis, R.E., Cahyame-Zuniga, L., Leventakos, K., Chamilos, G., Ben-Ami, R., Tamboli, P., Tarrand, J., Bodey, G.P., Luna, M., Kontoyiannis, D.P., 2013. Epidemiology and sites of involvement of invasive fungal infections in patients with haematological malignancies: a 20-year autopsy study. Mycoses 56, 638–645. doi:10.1111/myc.12081

Mattson, M.P., 2000. Apoptosis in neurodegenerative disorders. Nat. Rev. Mol. Cell Biol. 1, 120–130. doi:10.1038/35040009

Mayer, F.L., Wilson, D., Hube, B., 2013. Candida albicans pathogenicity mechanisms. Virulence 4, 119–128. doi:10.4161/viru.22913

Meriin, A.B., Zhang, X., He, X., Newnam, G.P., Chernoff, Y.O., Sherman, M.Y., 2002. Huntingtin toxicity in yeast model depends on polyglutamine aggregation mediated by a prion-like protein Rnq1. J. Cell Biol. 157, 997–1004. doi:10.1083/jcb.200112104

Portera-Cailliau, C., Hedreen, J.C., Price, D.L., Koliatsos, V., 1995. Evidence for apoptotic cell death in Huntington disease and excitotoxic animal models. J. Neurosci. 15, 3775–3787.

Richard, J.P., Melikov, K., Brooks, H., Prevot, P., Lebleu, B., Chernomordik, L.V., 2005. Cellular uptake of unconjugated TAT peptide involves clathrin-dependent endocytosis and heparan sulfate receptors. J. Biol. Chem. 280, 15300–15306. doi:10.1074/jbc.M401604200

Shi, R.-X., Ong, C.-N., Shen, H.-M., 2005. Protein kinase c inhibition and x-linked inhibitor of apoptosis protein degradation contribute to the sensitization effect of luteolin on tumor necrosis factor–related apoptosis-inducing ligand–induced apoptosis in cancer cells. Cancer Res. 65, 7815–7823. doi:10.1158/0008-5472.CAN-04-3875

Spincemaille, P., Alborzinia, H., Dekervel, J., Windmolders, P., van Pelt, J., Cassiman, D., Cheneval, O., Craik, D.J., Schur, J., Ott, I., 2014a. The plant decapeptide OSIP108 can alleviate mitochondrial dysfunction induced by cisplatin in human cells. Molecules 19, 15088–15102. doi:10.3390/molecules190915088

Spincemaille, P., Chandhok, G., Newcomb, B., Verbeek, J., Vriens, K., Zibert, A., Schmidt, H., Hannun, Y.A., van Pelt, J., Cassiman, D., 2014b. The plant decapeptide OSIP108 prevents copper-induced apoptosis in yeast and human cells. Biochim. Biophys. Acta BBA-Mol. Cell Res. 1843, 1207–1215. doi:10.1016/j.bbamcr.2014.03.004

Spincemaille, P., Pham, D.-H., Chandhok, G., Verbeek, J., Zibert, A., Libbrecht, L., Schmidt, H., Esguerra, C.V., de Witte, P.A., Cammue, B.P., 2014c. The plant decapeptide OSIP108 prevents copper-induced toxicity in various models for Wilson disease. Toxicol. Appl. Pharmacol. 280, 345–351. doi:10.1016/j.taap.2014.08.005

Strand, S., Hofmann, W.J., Grambihler, A., Hug, H., Volkmann, M., Otto, G., Wesch, H., Mariani, S.M., Hack, V., Stremmel, W., 1998. Hepatic failure and liver cell

damage in acute Wilson's disease involve CD95 (APO-1/Fas) mediated apoptosis. Nat. Med. 4, 588–593. doi:10.1038/nm0598-588

Thompson, C.B., 1995. Apoptosis in the pathogenesis and treatment of disease. Science 267, 1456–1462. doi:10.1126/science.7878464

Torcato, I.M., Huang, Y., Franquelim, H.G., Gaspar, D.D., Craik, D.J., Castanho, M.A., Henriques, S.T., 2013. The Antimicrobial Activity of Sub3 is Dependent on Membrane Binding and Cell-Penetrating Ability. ChemBioChem 14, 2013–2022. doi:10.1002/cbic.201300274

Verbandt, S., Cammue, B.P., Thevissen, K., 2016. Yeast as a model for the identification of novel survival-promoting compounds applicable to treat degenerative diseases. Mech. Ageing Dev. doi:10.1016/j.mad.2016.06.003

Winderickx, J., Delay, C., De Vos, A., Klinger, H., Pellens, K., Vanhelmont, T., Van Leuven, F., Zabrocki, P., 2008. Protein folding diseases and neurodegeneration: lessons learned from yeast. Biochim. Biophys. Acta BBA-Mol. Cell Res. 1783, 1381–1395. doi:10.1016/j.bbamcr.2008.01.020

FIGURES

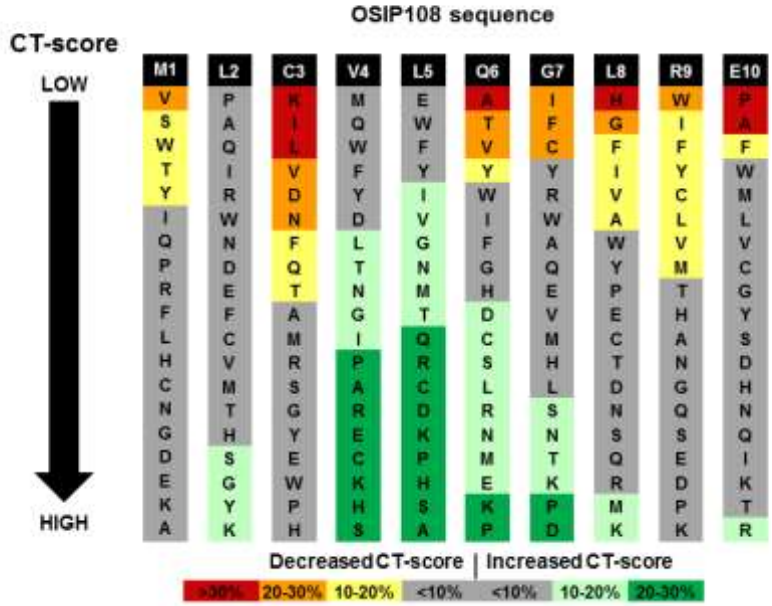

Figure 1. SAR study of OSIP108. Cisplatin tolerance (CT)-promoting activity of yeast treated with 100 µM of each OSIP108 variants in the presence of 250 µM cisplatin was determined. Variants are coloured based on the CT-score relative to treatment with OSIP108 in the same conditions. The OSIP108 sequence is shown in black. OSIP108 variants are ranked from the highest decrease (top) to the highest increase (bottom) in CT-score. Values are averages of three independent experiments, each with two technical replicates.

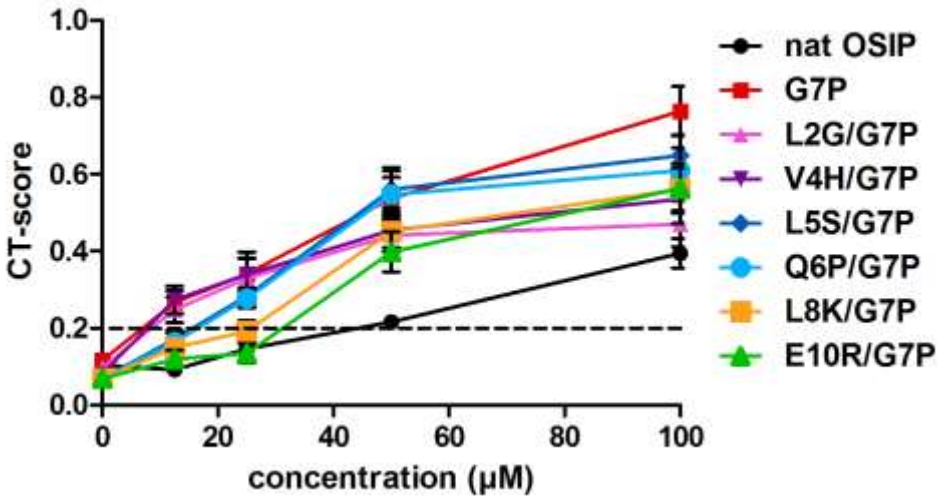

Figure 2. Dose response curves of OSIP108[G7P] double substituted variants. Dose response curves of cisplatin tolerance (CT)-promoting activity of different doses of OSIP108 (black line) and G7P variants (coloured lines). Yeast cultures were treated with peptide (12.5 µM- 100 µM) in presence of 250 µM cisplatin and incubated in the Bioscreen C plate reader. CT-scores are averages of at least three biologically independent experiments performed in duplicate. The dashed line at CT-score of 0.2 represents a two-fold increase in CT-score compared to the cisplatin-treated control, based on which MCT-2 values were calculated.

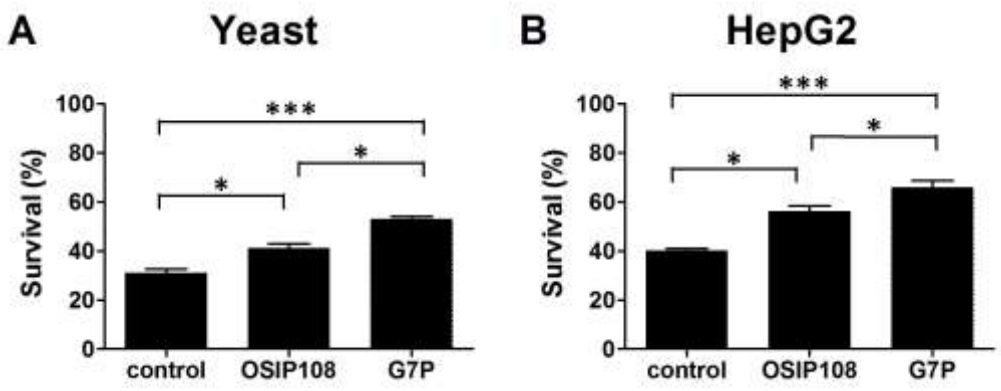

Figure 3. G7P increases survival of yeast and HepG2 cells in the presence of toxic copper. (A) Yeast cells were mock-treated (control 2% DMSO) or treated with 100 µM of either peptide (OSIP108 or the G7P variant) in the presence of $CuSO_4$ (1.75 mM). Survival (%) was calculated by determining CFUs of the copper-treated control as compared to the untreated control. (B) HepG2 cells were mock-treated (control 1% DMSO) or treated with 20 µM of either peptide (OSIP108 or the G7P variant) in presence of 0.75 mM $CuCl_2$. Subsequently, cell viability was determined by MTT staining and expressed relative to control-treated cells in absence of copper. Yeast experiments were performed in quadruplicate in four biological repeats, whereas HepG2 experiments were performed in triplicate in three biological repeats. (*$p<0.05$; ***$p<0.001$; ANOVA test using Bonferroni corrections).

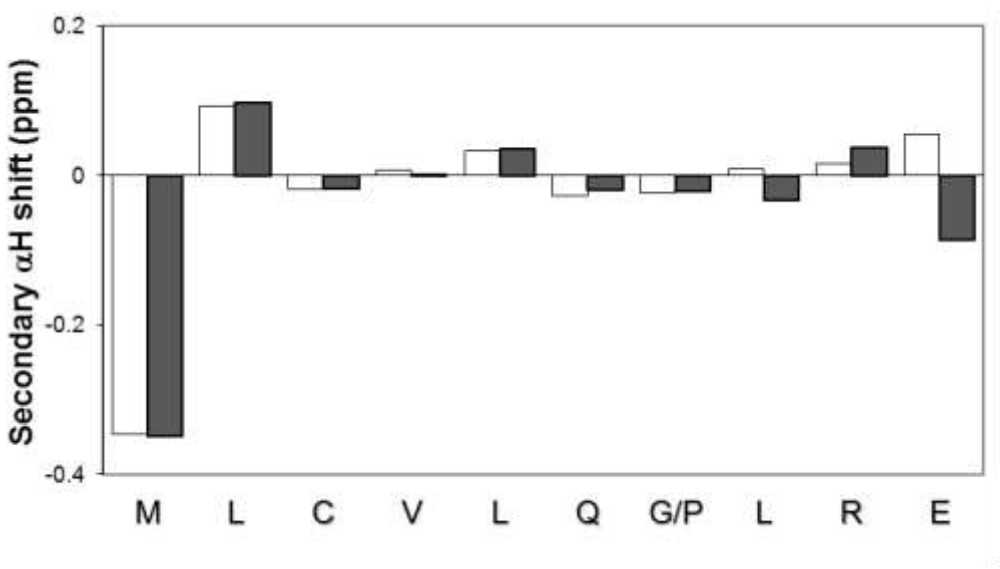

Figure 4. Secondary shift analysis of OSIP108 and OSIP108[G7P]. The amino acid sequence is displayed. White bars represent OSIP108; grey bars represent the G7P variant.

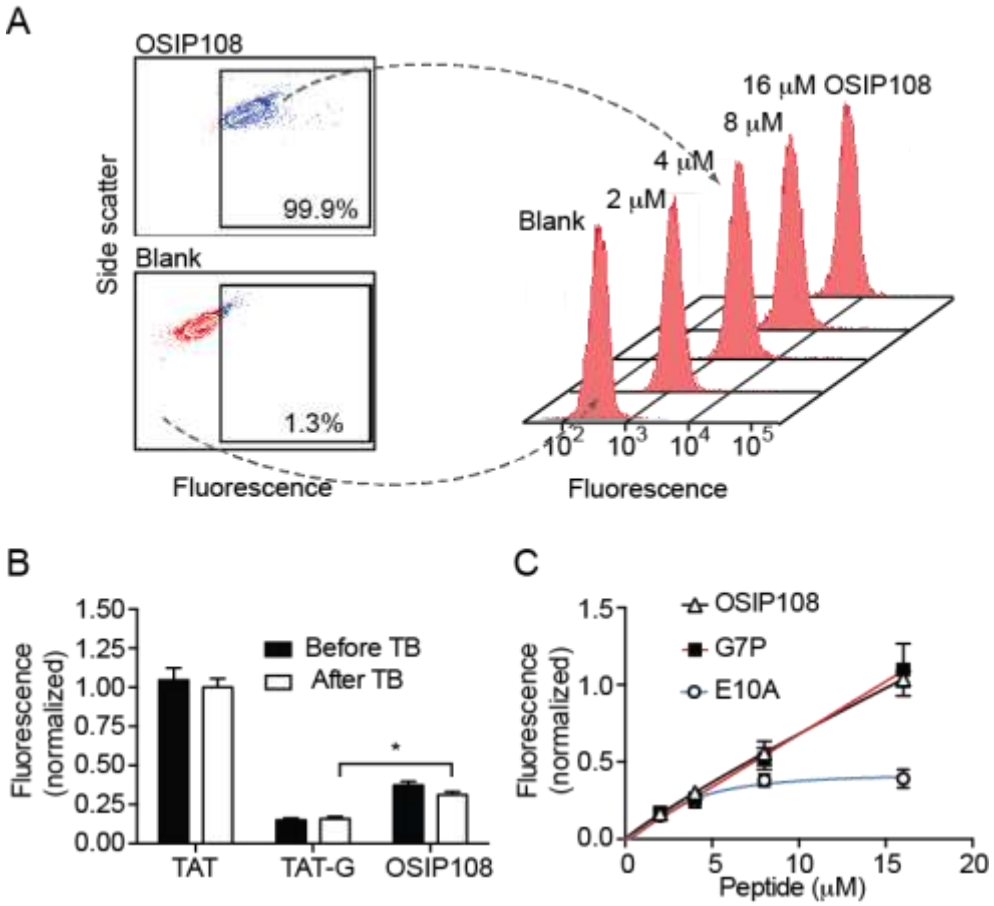

Figure 5. Internalization of OSIP108 and its variants into HeLa cells. Cells were incubated with fluorescently-labelled peptides for 1 h at 37ºC and the internalization was monitored by measuring the fluorescence emission intensity of Alexa Fluor®488 (excitation at 488 nm and emission at 530/30 nm) using flow cytometry. Fluorescence was measured before and after addition of the non-cell permeable quencher trypan blue (TB; 160 μg/mL); 10.000 cells were screened per sample. (A) Left panel, dotplots of the side scatter as a function of the fluorescence emission intensity of cells treated with 4 μM OSIP108 vs untreated cells (blank) obtained after addition of TB. Both axis are in log scale and the gate was drawn to exclude non-fluorescent cells. Virtually all the cells treated with 4 μM OSIP108 become fluorescent. Right panel, fluorescence emission intensity histograms of cells treated with varying concentrations of OSIP108. (B) Mean fluorescence emission intensity of cells treated with 4 μM of TAT, TAT-G

or OSIP108, before and after addition of TB. Fluorescence intensity was normalized for the average signal obtained with TAT after addition of TB. Data are represented as mean ± SEM of eight replicates. The statistical analysis was performed by one-way ANOVA by comparison with TAT-G after addition of TB (*$p < 0.05$). (C) Mean fluorescence emission intensity of cells treated with increasing concentrations of OSIP108, or of its variants E10A and G7P (4 µM- 16 µM). Fluorescence intensity was normalized for the average signal obtained with 4 µM TAT after addition of TB. Data are represented as mean ± SEM of three replicates.

TABLES

Table 1. Cisplatin tolerance (CT)-promoting activity of selected OSIP108 variants. OSIP108 variants with increased activity are further characterized by MCT-2, i.e. the minimum peptide concentration needed to increase CT by 2-fold compared to the cisplatin-treated control, and FC, i.e. fold change relative to OSIP108 (FC = MCT-2 OSIP108/MCT-2 OSIP108 variant). NA = not applicable. MCT-2 values for all peptide variants were significantly different from the MCT-2 of OSIP108 ($\alpha < 0.05$; one-way ANOVA test using Tukey post hoc analysis) except for the variants indicated with *. MCT-2 ± SEM are values of at least three biologically independent experiments with duplicate repeats.

OSIP108 variant	Sequence	MCT-2 ± SEM (μM)	FC	P value
OSIP108	MLCVLQGLRE	44.5 ± 3.4	NA	NA
L2G	M**G**CVLQGLRE	21.2 ± 3.8	2.1	0.00023
L2K	M**K**CVLQGLRE	21.3 ± 1.8	2.1	0.03273
L2Y	M**Y**CVLQGLRE	35.2 ± 1.7*	1.3	0.99982
V4H	MLC**H**LQGLRE	16.6 ± 1.7	2.7	0.00000
V4K	MLC**K**LQGLRE	27.1 ± 1.0*	1.6	0.39438
V4S	MLC**S**LQGLRE	21.8 ± 2.1	2.0	0.04320
L5A	MLCV**A**QGLRE	16.1 ± 0.5	2.8	0.01806
L5H	MLCV**H**QGLRE	16.7 ± 1.7	2.7	0.00192
L5S	MLCV**S**QGLRE	10.9 ± 0.8	4.1	0.00000
Q6E	MLCVL**E**GLRE	37.4 ± 3.9*	1.2	0.99998
Q6K	MLCVL**K**GLRE	25.9 ± 2.5*	1.7	0.11600
Q6P	MLCVL**P**GLRE	24.4 ± 5.3*	1.8	0.05235
G7D	MLCVLQ**D**LRE	21.4 ± 2.8	2.1	0.03417
G7K	MLCVLQ**K**LRE	21.5 ± 2.8	2.1	0.03634
G7P	MLCVLQ**P**LRE	9.2 ± 1.4	4.8	0.00000
L8K	MLCVLQG**K**RE	14.7 ± 1.7	3.0	0.00000
L8M	MLCVLQG**M**RE	14.9 ± 0.9	3.0	0.00980
E10R	MLCVLQGLR**R**	15.8 ± 3.7	1.8	0.00828
L2G/G7P	M**G**CVLQ**P**LRE	9.3 ± 0.9	4.8	0.00001
V4H/G7P	MLC**H**LQ**P**LRE	9.4 ± 1.0	4.8	0.00001
L5S/G7P	MLCV**S**Q**P**LRE	13.9 ± 2.0	3.2	0.00026
Q6P/G7P	MLCVL**PP**LRE	14.6 ± 2.0	3.1	0.00042
L8K/G7P	MLCVLQ**PK**RE	22.6 ± 4.3	2.0	0.06487
E10R/G7P	MLCVLQ**P**LR**R**	41.7 ± 6.0*	1.1	1.00000